FEBS Open Bio 4 (2014) 353–361

FEBS openbio

journal homepage: www.elsevier.com/locate/febsopenbio

Staphylococcal nuclease domain containing-1 (SND1) promotes migration and invasion via angiotensin II type 1 receptor (AT1R) and TGFβ signaling

Prasanna K. Santhekadur [a], Maaged Akiel [a], Luni Emdad [a], Rachel Gredler [a], Jyoti Srivastava [a], Devaraja Rajasekaran [a], Chadia L. Robertson [a], Nitai D. Mukhopadhyay [b], Paul B. Fisher [a,c,d], Devanand Sarkar [a,c,d,*]

[a] Department of Human and Molecular Genetics, Virginia Commonwealth University, Richmond, VA 23298, United States
[b] Department of Biostatistics, Virginia Commonwealth University, Richmond, VA 23298, United States
[c] Massey Cancer Center, Virginia Commonwealth University, Richmond, VA 23298, United States
[d] VCU Institute of Molecular Medicine, Virginia Commonwealth University, Richmond, VA 23298, United States

ARTICLE INFO

Article history:
Received 31 January 2014
Revised 13 March 2014
Accepted 27 March 2014

Keywords:
SND1
AT1R
TGFβ
PAI-1
Invasion

ABSTRACT

Staphylococcal nuclease domain containing-1 (SND1) is overexpressed in human hepatocellular carcinoma (HCC) patients and promotes tumorigenesis by human HCC cells. We now document that SND1 increases angiotensin II type 1 receptor (AT1R) levels by increasing AT1R mRNA stability. This results in activation of ERK, Smad2 and subsequently the TGFβ signaling pathway, promoting epithelial–mesenchymal transition (EMT) and migration and invasion by human HCC cells. A positive correlation was observed between SND1 and AT1R expression levels in human HCC patients. Small molecule inhibitors of SND1, alone or in combination with AT1R blockers, might be an effective therapeutic strategy for late-stage aggressive HCC.

1. Introduction

Hepatocellular carcinoma is the fifth most common cancer and the third most leading cause of cancer associated mortality in the world [1,2]. It is a highly aggressive disease and poses a major health problem because of its constantly increasing incidence and its poor prognosis owing to the lack of any effective treatment for the invasive and metastatic disease [2–4]. Its association with metabolic syndromes, such as diabetes, obesity, and non-alcoholic steatohepatitis (NASH), has made HCC an even major risk for life [5]. Elucidation of the molecular mechanism of aggressive HCC is the need of the time for developing molecular targeted therapies exerting lasting beneficial effect to the patients.

Staphylococcal nuclease domain containing-1 (SND1) is a multifaceted protein that regulates various intracellular processes, such as RNA interference as a nuclease in the RNA-induced silencing complex (RISC), mRNA splicing and stability, and transcription as a co-activator [6]. Recent studies have started to unravel the role of SND1 in carcinogenesis of diverse organs [7–11]. SND1 expression gradually increases with the stages and grades of cancer and its overexpression is associated with highly aggressive metastatic disease [9–11]. In our previous studies we documented that in 109 human HCC samples SND1 was overexpressed in ~74% cases compared to normal liver [11]. Correspondingly, in human HCC cells a significantly higher RISC activity was observed which was associated with increased degradation of tumor suppressor mRNAs that are target of oncomiRs thereby contributing to hepatocarcinogenesis [11]. Stable overexpression of SND1 augmented and siRNA-mediated inhibition of SND1 abrogated growth of human HCC cells in vitro and in vivo in nude mice xenograft studies [11]. SND1

Abbreviations: ACE, angiotensin-I converting enzyme; ACE-I, ACE inhibitors; AT1R, angiotensin II type 1 receptor; EMT, epithelial–mesenchymal transition; FDR, false discovery rate; HCC, human hepatocellular carcinoma; LP, losartan potassium; MTT, 3-(4,5-dimethylthiazol-2-yl)-2,5-diphenyltetrazolium bromide; NASH, non-alcoholic steatohepatitis; PAI-1, plasminogen activator inhibitor-1; RISC, RNA-induced silencing complex; SND1, Staphylococcal nuclease domain containing-1

* Corresponding author at: Department of Human and Molecular Genetics, Virginia Commonwealth University, 1220 East Broad St, PO Box 980035, Richmond, VA 23298, United States. Tel.: +1 (804) 827 2339; fax: +1 (804) 628 1176.
E-mail address: dsarkar@vcu.edu (D. Sarkar).

http://dx.doi.org/10.1016/j.fob.2014.03.012
2211-5463/

augmented tumor angiogenesis by activating NF-κB resulting in induction of miR-221 and angiogenic factors Angiogenin and CXCL16 [12]. These studies indicate that SND1 promotes aggressive HCC by multiple ways.

Angiotensin II (AngII), generated from angiotensin I (AngI) by angiotensin-I converting enzyme (ACE), and angiotensin II type 1 receptor (AT1R) play an important role in regulating hepatic fibrosis and eventual hepatocarcinogenesis by modulating functions of hepatic stellate cells [13–15]. AngII/AT1R has been shown to induce proliferation of human HCC cells via a cross-talk with epidermal growth factor receptor (EGFR) [16]. AngII also induces transforming growth factor-β (TGFβ) [17], a potent driver of cancer progression through the induction of epithelial–mesenchymal transition (EMT), in which epithelial cells acquire mesenchymal phenotype, leading to enhanced motility and invasion [18]. ACE inhibitors (ACE-I) and AT1R blockers demonstrated significant inhibitory effects on experimental murine liver fibrosis and HCC development [19,20]. A combination of ACE-I and vitamin K2 has been shown to significantly ameliorate cumulative recurrence of HCC [21].

In the present studies we document that SND1 increases AT1R level by augmenting AT1R mRNA stability leading to activation of TGFβ downstream signaling. The net effect of this pathway is induction of EMT contributing to increased migration and invasion by human HCC cells. We also document a positive correlation between SND1 and AT1R expression in human HCC patients. Inhibition of enzymatic activity of SND1 along with ACE-I and AT1R blockers might be an effective way to counteract a fatal malady like HCC.

2. Materials and methods

2.1. Cell lines and culture condition

Hep3B cells were obtained from ATCC and were cultured as recommended. The human HCC cell line QGY-7703, developed at Fudan University, Shanghai, was obtained from Dr. Zhao-zhong Su, and Huh7 cells were kindly provided by Dr. Paul Dent and were cultured as described [22]. The generation of the Hep3B-Con, Hep3B-SND1-17, Hep3B-SND1-9, QGY-Consi, QGY-SND1si-12 and QGY-SND1si-15 was described before [11,12]. Huh7 cells were transduced with a pool of three to five lentiviral vector plasmids, each encoding target-specific 19–25 nt (plus hairpin) shRNAs designed to knockdown SND1 gene expression (Santa Cruz Biotechnology). The cells were then selected for 2 weeks in 1 μg/ml puromycin and individual colonies (Huh7-SND1si) were isolated, expanded and maintained in 0.25 μg/ml puromycin. Similar strategy was used to generate Huh7-Consi clones. Hep3B-SND1-17 cells were transfected with plasmids expressing AT1R shRNA and stable clones (SND1-17-AT1Rsi) were generated by selection with 1 μg/ml puromycin. Similar strategy using control shRNA expressing plasmid was employed to generate SND1-17-Consi clones.

2.2. Chemicals and plasmids

Losartan potassium was obtained from Tocris Biosciences (Ellisville, MO, Catalogue# 3798) and used at a concentration of 10 μM. PD183452 was obtained from Sellecchem.com (Houston, TX, Catalogue# CI-1040) and used at a concentration of 20 μM. Recombinant human PAI-1 (Catalogue# 1786-PI-010) and TGFβ (Catalogue# 240-B-010) were obtained from R&D Systems (Minneapolis, MN) were used at concentrations of 20 and 1 nmol/ml, respectively. Actinomycin D was obtained from Sigma–Aldrich (St. Louis, MO, Catalogue# A1420) and used at a concentration of 5 μg/ml. Human PAI-1 promoter-luciferase reporter constructs, p800-luc and p549-luc, were kind gifts from Dr. Fahumiya Samad (Torrey Pines Institute for Molecular Studies, San Diego, CA). p800-luc contains −800 to +71 region of the promoter and p549-luc contains −549 to +71 region of the promoter lacking 2 SMAD, 1 AP-1 and 1 NF-κB binding sites compared to p800-luc [23]. Human AT1R (Catalogue# sc-29750) and PAI-1 (Catalogue# sc-36179) siRNAs and plasmids expressing scrambled shRNA (Catalogue# sc-108060) and AT1R shRNA plasmid (Catalogue# sc-29750-SH) were obtained from Santa Cruz Biotechnology (Santa Cruz, CA).

2.3. Migration assays

A wound healing/scratch assay was used to evaluate cell migration [24]. Confluent cells were scratched with a 200 μl micropipette tip to create a cell-free area. The scratched monolayers images were captured at 0 and 24 h after wounding using an Olympus IX-50 microscope equipped with a Variocam camera. Cell migration distance was determined by measuring the wound width and subtracting this from the initial value using ImageJ software. A total of six areas were randomly selected in each well, and the cells in three wells of either group were quantified in each experiment. Cells were treated with rPAI-1, TGFβ, LP or PD183452 for 24 h before scratch was made. Cells were transfected with PAI-1 siRNA, plated on 6-well plates after 24 h and scratch was made after another 24 h.

2.4. Invasion assays

Invasion was measured by using 24-well BioCoat cell culture inserts with an 8-μ-porosity polyethyleneterepthalate membrane coated with Matrigel basement membrane matrix (100 μg/cm^2) (BD Biosciences, Franklin Lakes, NJ) [22]. Briefly, the Matrigel was allowed to rehydrate for 2 h at room temperature by adding warm, serum-free DMEM. The wells of the lower chamber were filled with medium containing 5% FBS. Cells (5×10^4) were seeded in the upper compartment (6.25-mm membrane size) in serum-free medium. The invasion assay was performed at 37 °C in a 5% CO_2 humidified incubator for 22 h. At the end of the invasion assay, the filters were removed, fixed, and stained with the Diff-Quick staining kit. Cells on the upper surface of the filters were removed by wiping with a cotton swab, and invasion was determined by counting the number of cells that migrate to the lower side of the filter with a microscope at 100× magnification. Cells were treated with rPAI-1 (20 nmol/ml), TGFβ (1 nmol/ml), losartan potassium (LP, 10 μM) or PD183452 (20 μM) for 24 h before plating on the invasion chamber. Cells were transfected with PAI-1 siRNA and 48 h later plated on the invasion chamber.

2.5. Tissue microarray and immunohistochemistry

Human HCC tissue microarray, containing 40 primary HCC, 10 metastatic HCC and 9 normal adjacent liver samples was obtained from Imgenex Corp (San Diego, CA, Catalogue# IMH-360) [22]. Out of the 50 HCC samples, 14 belongs to Stage I, 9 belongs to Stage II, 14 belongs to Stage III and 13 belongs to Stage IV. Following deparaffinization, the sections were permeabilized with a 0.1% TritonX-100 solution in PBS for 30 min. Sections were then blocked for 1 h at room temperature with 2% goat serum and 1% BSA in PBS and incubated with anti-SND1 antibody (rabbit polyclonal; 1:100; Prestige Antibodies® Powered by Atlas Antibodies from Sigma) or anti-AT1R antibody (1:200; rabbit polyclonal; Abnova) overnight at 4 °C. Sections were then rinsed in PBS, and incubated with anti-rabbit secondary antibody for 1 h at room temperature. The signals were developed by avidin–biotin–peroxidase complexes with a DAB substrate solution (Vector laboratories). The images were taken by an Olympus microscope.

2.6. Preparation of whole cell lysates and Western blot analyses

Preparation of whole cell lysates and Western blot analyses were performed as described [22]. The following rabbit primary antibodies were obtained from Cell signaling Technology (Danver, MA) and used at a dilution of 1:1000: E-cadherin (#4065), N-cadherin (#4061), Slug (C19G7 monoclonal, #9585), Snail (C15D3 monoclonal, #3879), Vimentin (R28, #3932), phospho-p44/42 MAPK (Erk1/2, #4370), p44/42 MAPK (Erk1/2, #4695), phospho-SMAD2 (#3104) and SMAD2/3 (D7G7 monoclonal, #8685). The other primary antibodies used were SND1 (rabbit polyclonal, 1:1000, Sigma), AT1R (rabbit polyclonal, 1:1000, Abnova), GAPDH (rabbit polyclonal, 1:1000, Santa Cruz), β-actin (mouse monoclonal, 1:2000, Sigma) and EF1-α (mouse monoclonal, 1:1000, Millipore). Densitometric analysis was performed by ImageJ software.

2.7. Cell viability and clonogenic assays

Cell viability was determined by standard 3-(4,5-dimethylthiazol-2-yl)-2,5-diphenyltetrazolium bromide (MTT) assays as described [22]. For colony formation assay, cells (1×10^3) were plated in 6-cm dishes and colonies >50 cells were counted after 2 weeks [22].

2.8. Total RNA extraction, real time PCR and Affymetrix microarray

Total RNA was extracted using Qiagen miRNAeasy mini kit (Qiagen, Valencia, CA). Real time PCR was performed using an ABI 7900 fast real time PCR system and Taqman gene expression assays for AT1R and GAPDH according to the manufacturer's protocol (Life Technologies). Total RNA was used to perform Affymetrix Oligonucleotide Microarray (Human U133 plus 2.0) between QGY-Consi versus QGY-SND1si-12 and QGY-SND1si-15 clones according to the manufacturer's instructions. The standard Affymetrix® protocol was used for generation of fragmented labeled cRNA for hybridization. The HG-U133A 2.0 array provides comprehensive coverage of the transcribed human genome by including 22,277 probe sets that analyze the expression level of over 18,400 human transcripts. Data analysis was performed as described [25]. The data have been submitted to GEO with accession number GSE44601. The expression of genes that showed a false discovery rate (FDR; q-value) 0 and p-value <0.001 was presented in Table S1.

2.9. Human angiogenesis array

The expression levels of 55 angiogenesis associated proteins were analyzed using conditioned media from cells cultured in serum-free condition with the Human Angiogenesis Antibody Array kit (R&D Systems, Proteome Profiler TM) as recommended by the manufacturer [12]. The cells were pretreated with PD183452 for 2 h.

2.10. Enzyme-linked immunosorbent assay (ELISA)

The expression of TGFβ and PAI-1 were analyzed in conditioned media using ELISA kits (R&D Systems, Quantakine R) as recommended by the manufacturer. Cells were transfected with AT1R siRNA, 48 h later medium was replaced by serum-free media to which LP was added and PAI-1 level was measured after 24 h.

2.11. Transient transfection and luciferase assays

Cells (1×10^5) were plated in each well of a 24-well tissue culture plate. Next day transfection was performed using Lipofectamine® 2000 Reagent (Life Technologies, Grand Island, NY) with 950 ng of luciferase reporter plasmid and 50 ng of Renilla luciferase plasmid as internal control for each well. The cells were treated or not with TGFβ (1 nmol/ml) for 48 h. Luciferase activity was measured using a Dual Luciferase Reporter Assay kit (Promega, Madison, WI) according to the manufacturer's protocol and firefly luciferase activity was normalized by Renilla luciferase activity.

2.12. Statistical analysis

Data were represented as the mean ± Standard Error of Mean (S.E.M) and analyzed for statistical significance using one-way analysis of variance (ANOVA) followed by Newman–Keuls test as a post hoc test. To assess the strength of association between SND1 and AT1R an ordinal logistic regression was conducted with SND1 expression Pearson's χ^2 goodness of fit test with 6 degrees of freedom was performed.

3. Results

3.1. SND1 promotes migration and invasion of human HCC cells

We previously documented that Hep3B and QGY-7703 cells express low and high levels of SND1, respectively [11]. Stable overexpression of SND1 in Hep3B cells significantly augments while stable knockdown of SND1 in QGY-7703 cells significantly inhibits in vitro proliferation, angiogenesis and formation of subcutaneous xenografts in athymic nude mice [11,12]. These findings were observed in multiple clones of SND1-overexpressing Hep3B cells as well as SND1-knockdown QGY-7703 cells and these clones have been characterized in detail [11,12]. In the present study we employed these clones as well as clones of Huh7 cells, which express high level of SND1, with stable knockdown of SND1. Stable overexpression of SND1 in Hep3B cells induced a morphological change with elongated, spindle-shaped, fibroblast-like cells while stable knockdown of SND1 in QGY-7703 and Huh7 cells induced a blunted morphology (Fig. 1A) suggesting that SND1 might affect cell motility and thereby migration and invasion, two major determinants of an aggressive cancer. To analyze migration and invasion, we performed wound healing assay and Matrigel invasion assay, respectively, using the established clones. A significant increase in migration and invasion was observed in SND1 overexpressing Hep3B-SND1-17 clone compared to the control Hep3B clone (Hep3B-Con) (Fig. 1B and C). As a corollary a significant decrease in migration and invasion was observed in SND1 knockdown clones QGY-SND1si-12 and Huh7-SND1si-7 when compared to the control clones QGY-Consi and Huh7-Consi, expressing control siRNA, respectively (Fig. 1B and C). Similar finding was observed in additional SND1-overexpressing and SND1 knockdown clones (Fig. S1).

3.2. SND1 modulates TGFβ signaling pathway

To get an insight into the molecular mechanism by which SND1 modulates migration and invasion gene expression profiles were compared between QGY-Consi versus QGY-SND1si-12 and QGY-SND1si-15 clones by Affymetrix oligonucleotide microarray (Human U133 plus 2.0). We focused on those genes that were downregulated in SND1 knockdown clones compared to the control clone. Using a q-value of 0, we observed significant downregulation of 123 genes upon SND1 knockdown (Table S1). Interestingly we observed significant downregulation of several Transforming Growth Factor β (TGFβ) downstream genes, such as TAGLN, NUPR1, IGFBP3 and KLF6 [26], in SND1 knockdown clones compared to the control clones. Since TGFβ is a known regulator of cell motility, migration and epithelial–mesenchymal transition (EMT) [18] we focused our work on unraveling the role of TGFβ in SND1-mediated augmentation of migration and invasion as well

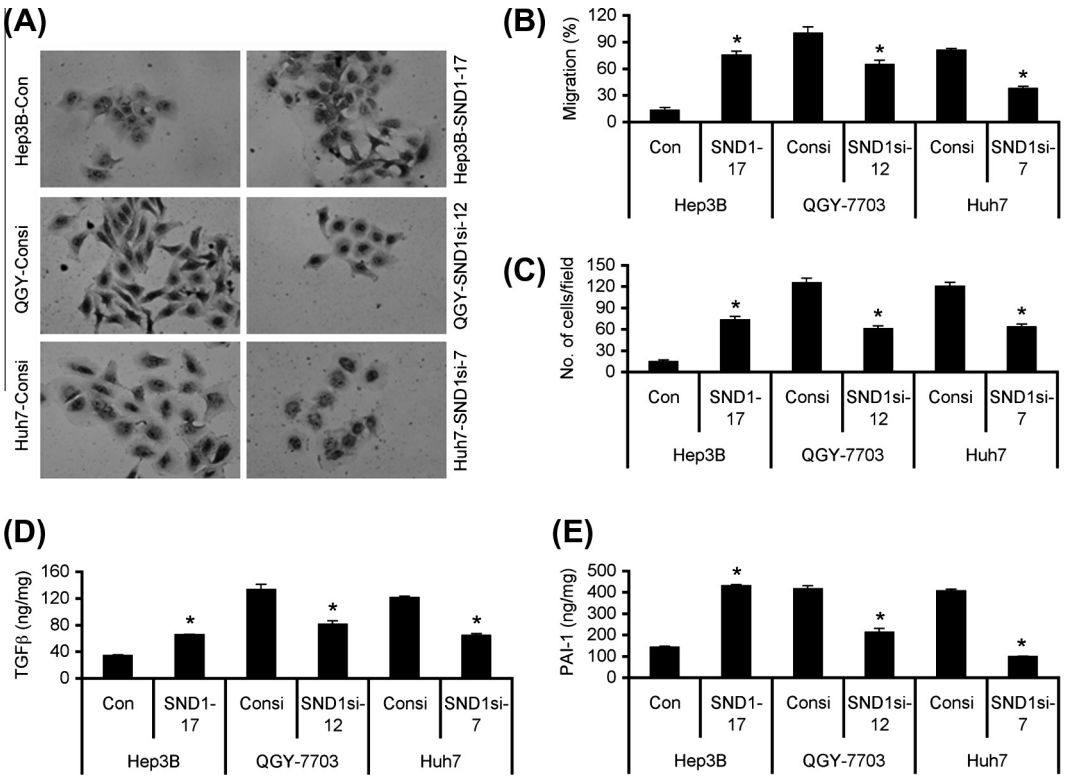

Fig. 1. SND1 promotes migration and invasion of human HCC cells. (A) Photomicrograph of the indicated cells, magnification 200×. (B) Graphical representation of the migration ability of the indicated cells when the migration ability of QGY-Consi clone was considered as 100%. (C) Graphical representation of the Matrigel invasion assay performed in the indicated cells. (D and E) TGFβ (D) and PAI-1 (E) levels in the conditioned media of the indicated cells determined by ELISA. For B–E, data represent mean ± SEM of 3 independent experiments. * $p < 0.01$.

as the mechanism of TGFβ induction by SND1. Our findings were bolstered by our previous observations using an angiogenesis array that SND1 significantly induces Plasminogen Activator Inhibitor-1 (PAI-1) [12], a known TGFβ-downstream gene promoting migration and invasion of tumor cells [27].

We first confirmed regulation of TGFβ and PAI-1 by SND1 by determining TGFβ and PAI-1 levels in conditioned media of SND1 overexpressing and SND1 knockdown clones using ELISA. Indeed, TGFβ and PAI-1 levels were significantly increased in Hep3B-SND1-17 clone compared to Hep3B-Con clone while those levels were significantly decreased in QGY-SND1si-12 and Huh7-SND1si-7 clones compared to QGY-Consi and Huh7-Consi clones, respectively (Fig. 1D and E). Knocking down PAI-1 by siRNA in Hep3B-SND1-17 clone and QGY-7703 cells significantly decreased migration and invasion while treatment of Hep3B and QGY-SND1si-12 cells with recombinant PAI-1 significantly increased migration and invasion (Fig. 2A–F). As a corollary treatment with TGFβ significantly increased migration and invasion of Hep3B cells and QGY-SND1si-12 clone (Fig. 2C–F). Since TGFβ is a known regulator of epithelial-mesenchymal transition (EMT) we checked the expression of EMT markers in these clones. The level of E-cadherin did not change significantly upon SND1 overexpression in Hep3B cells while it was not detected in QGY-7703 cells (Fig. 2G). However, E-cadherin level increased significantly in Huh7-SND1si-7 clone when compared to parental Huh7 cells or Huh7-Consi clone (Fig. 2G). The levels of N-cadherin, Slug, Snail and Vimentin increased significantly in Hep3B-SND1-17 clone when compared to Hep3B-Con clone while those levels decreased significantly in QGY-SND1si-12 and Huh7-SND1si-7 clones when compared to QGY-Consi and Huh7-Consi clones, respectively, indicating that SND1 plays an important role in regulating EMT (Fig. 2G).

To check transcriptional regulation of PAI-1 by SND1 and TGFβ we analyzed PAI-1 promoter-luciferase activity using two reporter constructs, p800-luc containing −800 to +71 region of the promoter and p549-luc containing −549 to +71 region of the promoter [23]. p549-luc construct lacks 2 SMAD, 1 AP-1 and 1 NF-κB binding sites compared to p800-luc [23]. Under basal condition the activity of p800-luc showed 2-fold induction in Hep3B-SND1-17 clone when compared to Hep3B-Con clone (Fig. 2H). Upon TGFβ treatment p800-luc activity increased by 85-fold in Hep3B-Con clone while a 291-fold increase was observed in Hep3B-SND1-17 clone. Under basal condition no significant difference was observed in p549-luc activity between Hep3B-Con and Hep3B-SND1-17 clones. Upon TGFβ treatment p549-luc activity increased by 9-fold in Hep3B-Con clone while a 17-fold increase was observed in Hep3B-SND1-17 clone. The augmented activity of p800-luc and the marked attenuation of the activity of p549-luc by SND1 and TGFβ indicate that SND1 and TGFβ regulate PAI-1 expression by modulating its transcription.

3.3. SND1 induces TGFβ expression through AT1R signaling

We next sought for the molecular mechanism by which SND1 induces TGFβ. Angiotensin II type 1 receptor (AT1R) induces TGFβ expression and previous studies have documented that SND1 increases AT1R level by augmenting AT1R mRNA stability [28]. We observed that AT1R protein level was significantly increased in Hep3B-SND1-17 clone compared to Hep3B-Con clone and was significantly downregulated in QGY-SND1si-12 and Huh7-SND1si-7 clones when compared to QGY-Consi and Huh7-Consi clones, respectively (Fig. 3A). Extracellular signal-regulated kinase (ERK) and SMAD2 are downstream signal transduction molecule from AT1R. Indeed, we observed increased activation of ERK and

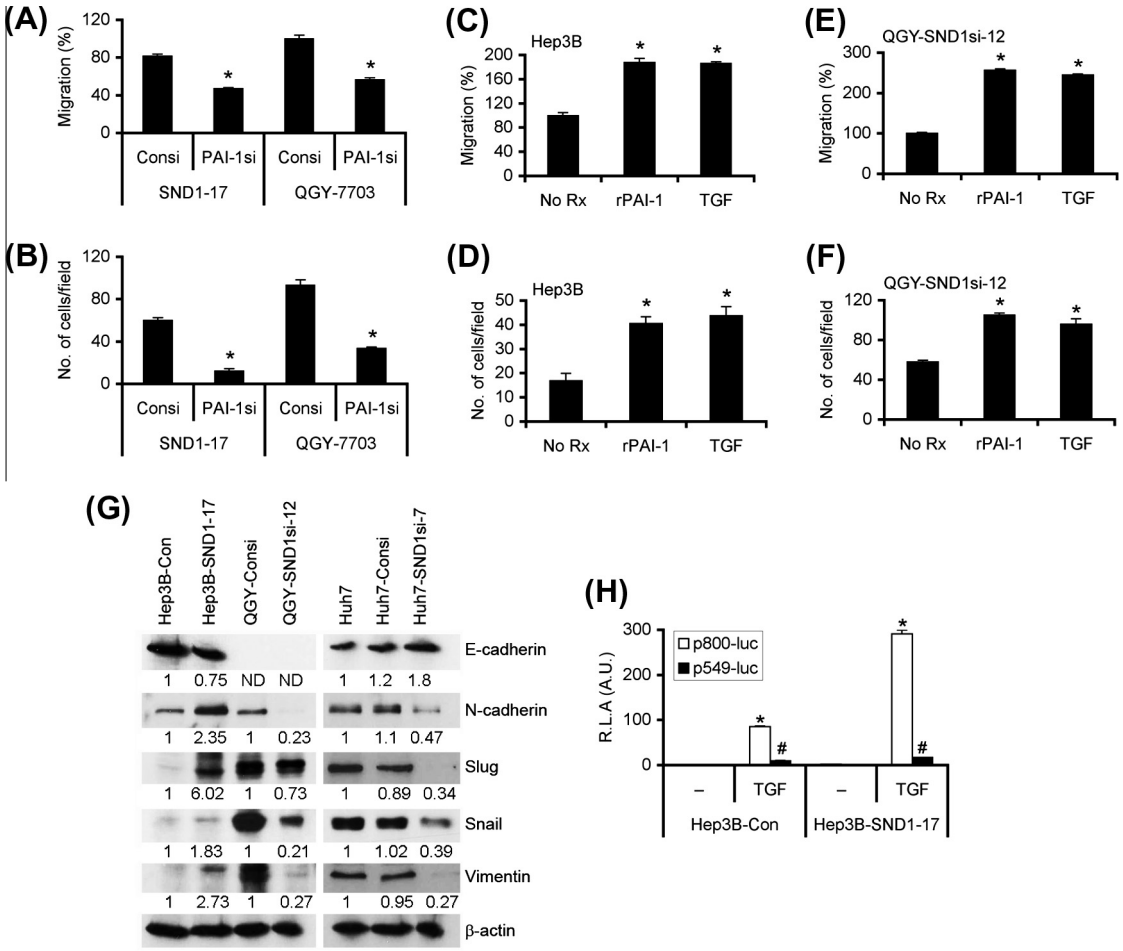

Fig. 2. PAI-1 and TGFβ promote migration and invasion of human HCC cells. (A and B) Hep3B-SND1-17 and QGY-7703 cells were transfected with either control scrambled siRNA or PAI-1 siRNA and then subjected to migration (A) and Matrigel invasion (B) assay. (C and D) Hep3B cells were treated with recombinant PAI-1 or TGFβ and migration (C) and invasion (D) assays were performed. Migration ability of untreated Hep3B cells was considered as 100%. (E and F) QGY-SND1si-12 cells were treated with recombinant PAI-1 (20 nmol/ml) or TGFβ (1 nmol/ml) and migration (E) and invasion (F) assays were performed. Migration ability of untreated QGY-SND1si-12 cells was considered as 100%. For A–F, data represent mean ± SEM of 3 independent experiments. $^{*}p < 0.01$. (G) Analysis of the expression of the indicated markers of EMT in the indicated cells by Western blot. β-actin was used as loading control. The numbers indicate densitometric quantification when the level of each protein was divided by the level of β-actin and the normalized levels in Hep3B-Con, QGY-Consi and Huh7 were considered as 1. (H) Analysis of human PAI-1 promoter luciferase activity using p800-luc and p549-luc in the indicated cells. R.L.A.: relative luciferase activity. A.U.: arbitrary units of fold change when the luciferase activity of p800-luc in Hep3B-Con cells was considered as 1. Data represent mean ± SEM of 3 independent experiments. $^{*}p < 0.01$ vs no treatment, $^{\#}p < 0.01$ vs p800-luc.

SMAD2 in Hep3B-SND1-17 clone compared to Hep3B-Con clone and decreased activation in QGY-SND1si-12 and Huh7-SND1si-7 clones when compared to QGY-Consi and Huh7-Consi clones, respectively, indicating that overexpression of AT1R might lead to functional AT1R signaling (Fig. 3A). To confirm that SND1 increases AT1R protein level by elevating AT1R mRNA stability we treated Hep3B-Con, Hep3B-SND1-17 and Hep3B-SND1-9 clones with Actinomycin D to shut down transcription and determined AT1R mRNA level temporally. Under basal condition AT1R mRNA level was significantly higher in Hep3B-SND1-17 and Hep3B-SND1-9 clones compared to Hep3B-Con clone (Fig. 3B). Upon Actinomycin D treatment, at 4 h, AT1R mRNA level decreased by 50% in Hep3B-Con clone while the level decreased by only 15% in SND1-overexpressing clones (Fig. 3C) indicating that increased stability of AT1R mRNA, conferred by SND1, might contribute to increased AT1R protein level.

We analyzed SND1 and AT1R expression by immunohistochemistry in a tissue microarray containing 50 human HCC samples and 9 matched normal liver samples. A representative result from one patient is shown in Fig. 3D. SND1 expression was virtually undetectable in normal human liver while its expression was markedly higher in the HCC samples. Constitutive low level expression of AT1R was detected in normal liver. However, its expression was significantly higher in the HCC samples. A statistically significant correlation ($p < 0.0001$) was observed between SND1 and AT1R levels in these patients using a Pearson's χ^2 goodness of fit test with 6 degrees of freedom further establishing the regulation of AT1R by SND1 in the clinical situation (Fig. 3E).

To investigate the role of AT1R in mediating SND1-induced migration and invasion we blocked AT1R using a specific chemical inhibitor Losartan potassium (LP). Treatment of Hep3B-SND1-17, QGY-7703 and Huh7 cells with LP (10 μM) significantly inhibited both migration and invasion (Fig. 4A and B). As a corollary, treatment of Hep3B-SND1-17 and QGY-7703 cells with either AT1R siRNA or LP significantly inhibited PAI-1 expression while a combination of AT1R siRNA and LP resulted in further inhibition in PAI-1 level indicating the involvement of AT1R in regulating SND1-induced PAI-1 expression (Fig. 4C). It should be noted that treatment of SND1-overexpressing and SND1-knockdown clones with LP for 5 days did not significantly affect cell viability as measured by standard MTT assay (Fig. 4D). However, in a 2-week long clonogenic assay, LP treatment inhibited colony formation mod-

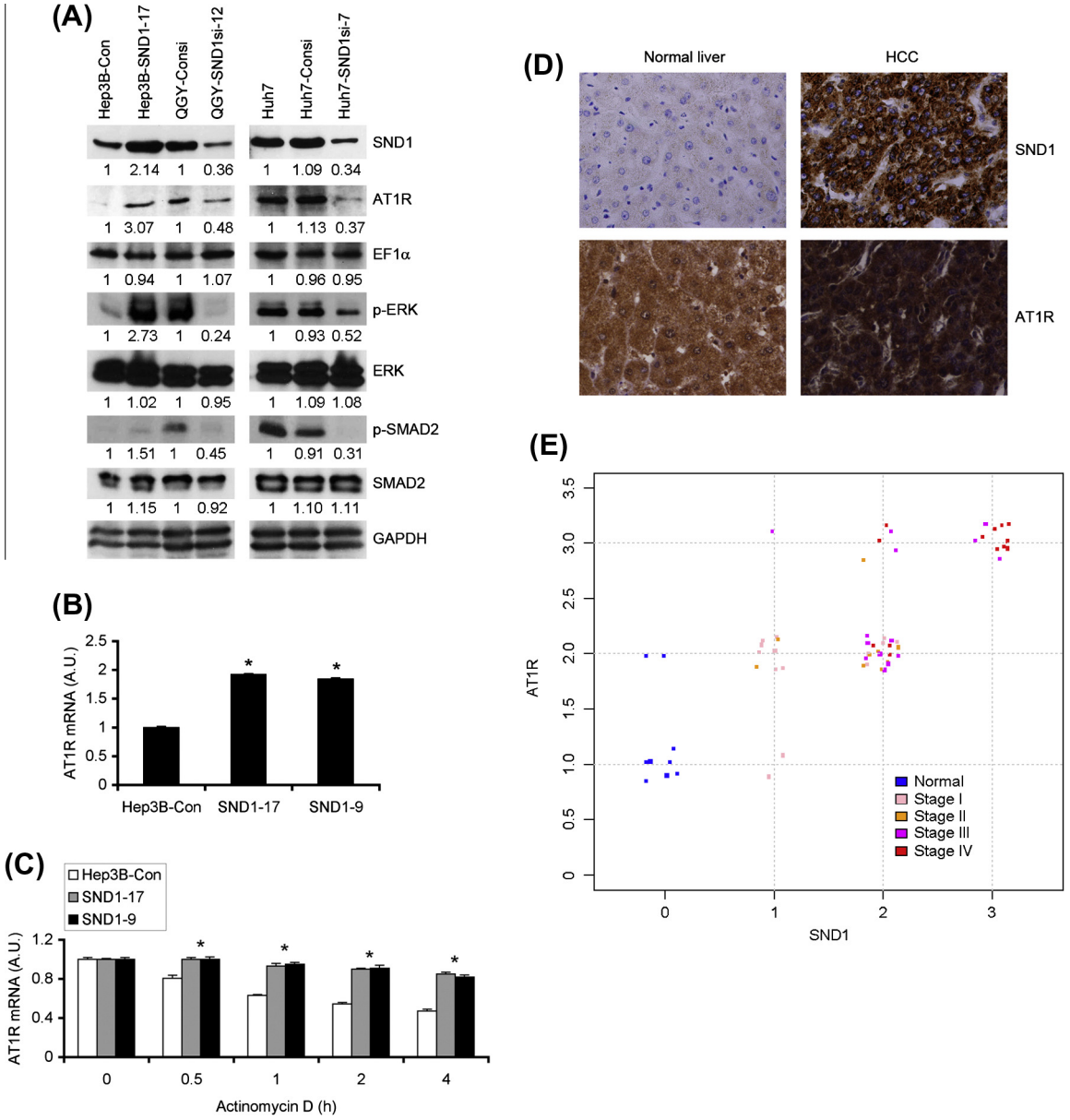

Fig. 3. AT1R is induced by SND1. (A) Analysis of the expression of the indicated proteins in the indicated cells by Western blot. EF1α and GAPDH were used as loading control. The numbers indicate densitometric quantification when the level of each protein was divided by the level of GAPDH and the normalized levels in Hep3B-Con, QGY-Consi and Huh7 were considered as 1. (B) Basal AT1R mRNA level in the indicated cells determined by Taqman RT-PCR. A.U.: arbitrary units of fold change when AT1R mRNA level in Hep3B-Con cells was considered as 1. (C) Hep3B-Con, Hep3B-SND1-17 and Hep3B-SND1-9 clones were treated with actinomycin D (5 μg/ml) for the indicated time point and AT1R mRNA level was determined by Taqman RT-PCR. A.U.: arbitrary units of fold change when AT1R mRNA level in Hep3B-Con cells at 0 time point was considered as 1. Data represent mean ± SEM of 3 independent experiments. $^{*}p < 0.01$. (D) Immunohistochemical analysis of SND1 and AT1R in normal liver and HCC samples, magnification 400×. (E) Graph representing coexpression of SND1 and AT1R in normal liver and HCC of all stages. $p < 0.0001$ by Pearson's χ^2 goodness of fit test with 6 degrees of freedom.

estly but significantly (Fig. 4E). Collectively, these findings suggest that AT1R-mediated signaling mainly regulates SND1-induced cell motility rather than viability and proliferation.

To further confirm the importance of AT1R in SND1 function we established stable clones in the background of Hep3B-SND1-17 clone expressing AT1R siRNA. Compared to the control clones, Consi-1 and Consi-2 stably expressing control, scrambled siRNA, two independent AT1R siRNA expressing clones, AT1Rsi-3 and AT1Rsi-12, showed significantly decreased level of AT1R with corresponding decreased activation of ERK and SMAD2 (Fig. 5A). AT1Rsi-3 and AT1Rsi-12 clones of Hep3B-SND1-17 clone showed significantly decreased migration (Fig. 5B), invasion (Fig. 5C), and PAI-1 (Fig. 5D) and TGFβ (Fig. 5E) expression, when compared to Consi-1 and Consi-2 clones.

3.4. ERK mediates SND1-induced migration and invasion

Since ERK activation is markedly augmented by SND1 we next checked the effect of ERK inhibition by PD184352 on SND1-induced migration and invasion. Treatment of Hep3B-SND1-17, QGY-7703 and Huh7 cells with PD184532 (20 μM) significantly inhibited both migration and invasion (Fig. 6A and B). Treatment of Hep3B-SND1-17 and QGY-7703 cells with PD184532 significantly inhibited PAI-1 expression (Fig. 6C). These findings were extended further by treating Hep3B-SND1-17 clone with PD184532 for 2 h in serum-free medium and then using the conditioned media for a protein array that detects 55 proteins regulating invasion, angiogenesis and metastasis. PD184532 treatment resulted in significant downregulation of 11 proteins, including

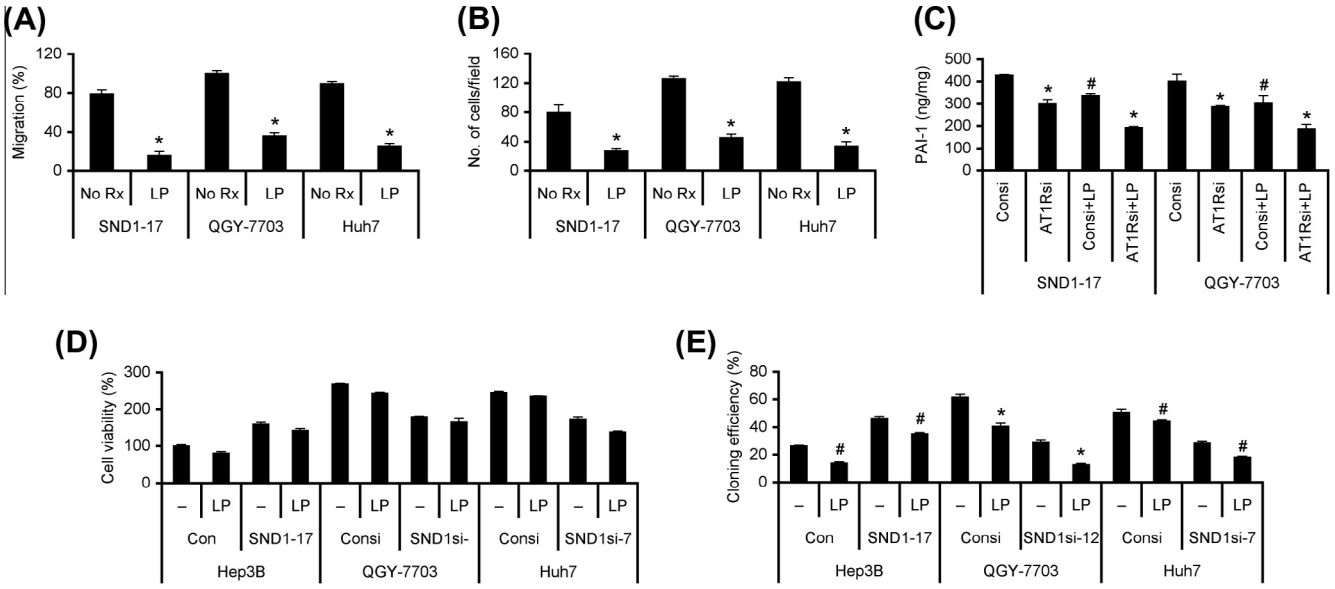

Fig. 4. Chemical inhibition of AT1R abrogates migration and invasion by human HCC cells. (A and B) The indicated cells were treated with losartan potassium (LP; 10 μM) and migration (A) and Matrigel invasion (B) were analyzed. (C) The indicated cells were transfected with either control, scrambled siRNA or AT1R siRNA and treated or not with LP and PAI-1 level in the conditioned media was determined by ELISA. (D) The indicated cells were treated with LP for 5 days and cell viability was determined by standard MTT assay. Cell viability of untreated Hep3B-Con clone was considered as 100%. (E) The indicated cells were treated with LP for 2 weeks and clonogenic assay was performed. For A–E, data represent mean ± SEM of 3 independent experiments. $^{*}p < 0.01$.

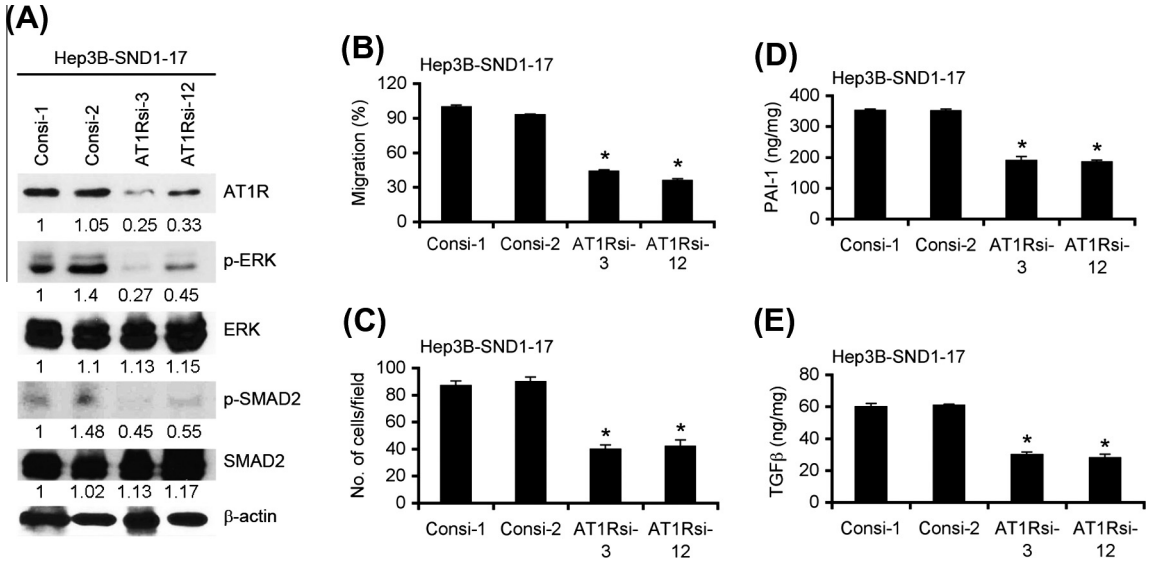

Fig. 5. Genetic inhibition of AT1R abrogates migration and invasion by human HCC cells. Consi-1 and Consi-2 are stable clones of Hep3B-SND1-17 clone expressing control, scrambled shRNA. AT1Rsi-3 and AT1Rsi-12 are stable clones of Hep3B-SND1-17 clone expressing AT1R shRNA. (A) The expression of the indicated proteins were determined in the indicated cells by Western blot. β-actin was used as loading control. The numbers indicate densitometric quantification when the level of each protein was divided by the level of β-actin and the normalized level in Consi-1 was considered as 1. (B and C) Migration (B) and Matrigel invasion (C) assays were performed in the indicated clones. (D and E) PAI-1 (D) and TGFβ (E) levels were determined in the conditioned media of the indicated cells. For B–E, data represent mean ± SEM of 3 independent experiments. $^{*}p < 0.01$.

PAI-1 (Fig. 6D and S2). The combined downregulation of these regulatory factors by PD184532 indicates the importance of ERK in mediating SND1-induced invasion, angiogenesis and metastasis.

4. Discussion

Although the role of AngII/AT1R is well-established in hepatic fibrosis via modulating HSC and in tumor angiogenesis by regulating functions of endothelial cells, the contribution of this signaling pathway to regulate other aspects of hepatocarcinogenesis has not been clearly demonstrated. In the present studies we delineate a novel molecular mechanism linking SND1 and AT1R with subsequent activation of TGFβ signaling contributing to EMT and migration and invasion by human HCC cells. These findings extend our previous observation that SND1 augments tumor angiogenesis through NF-κB, miR-221, Angiogenein, and CXCL16 [12]. SND1 thus contributes to all the hallmarks of cancer by multiple mechanisms inducing a highly aggressive cancer.

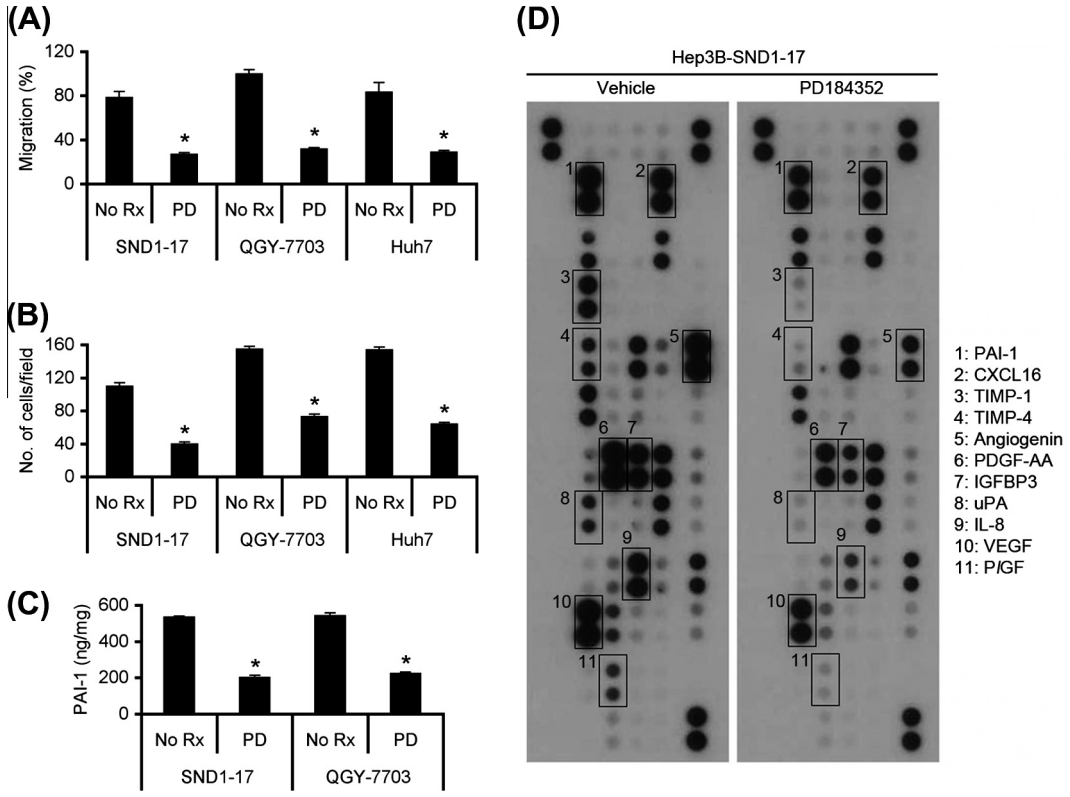

Fig. 6. Inhibition of ERK abrogates migration and invasion by human HCC cells. (A and B) The indicated cells were treated with PD183452 (20 μM) and were subjected to migration (A) and Matrigel invasion (B) assays. (C) The indicated cells were treated with PD183452 and PAI-1 level in the conditioned media was determined by ELISA. (D) Hep3B-SND1-17 cells were treated with PD183452 and the conditioned media was used for a protein array. For A–C, data represent mean ± SEM of 3 independent experiments. $^{*}p < 0.01$.

Previous studies have documented that SND1 binds to the 3′-untranslated region (3′-UTR) of AT1R mRNA via the nuclease domains resulting in increased AT1R expression by decreasing the rate of mRNA decay and enhancing translation [28]. This function of SND1 is independent of its function in RISC where it facilitates mRNA degradation [28,29]. We also document that the level of AT1R protein is increased in SND1-overexpressing cells and decreased in SND1-knockdown cells and our mRNA stability studies using actinomycin D clearly demonstrates increased half-life of AT1R mRNA in SND1-overexpressing clones compared to control clone. As yet AT1R overexpression in human HCC patients has not been documented and we observed a significant statistical correlation between SND1 and AT1R levels in HCC samples versus normal liver. Thus a post-transcriptional regulation of AT1R by SND1 might play an important role in promoting aggressive progression of HCC. This overexpression of AT1R might lead to its constitutive activation since we observed activation of downstream signaling pathways without addition of natural AT1R ligand angiotensin II. The factors that determine whether SND1 will function as a component of RISC or promote mRNA stability remain to be identified. Search for a SND1 recognition motif, present in AT1R 3′-UTR, in other mRNAs might identify additional SND1 targets and provide an explanation of preferential selection of SND1 in executing its function.

There might be multiple ways by which SND1 regulates TGFβ signaling cascade. TGFβ signaling through TGFβR1 promotes tumorigenesis while that through TGFβR2 functions as a tumor suppressor [30]. We previously documented that as part of RISC SND1 promotes degradation of TGFβR2 mRNA, a target of the oncogenic miRNA-93, thus facilitating the oncogenic TGFβ/TGFβR1 signaling [11]. A promoter microarray study based on chromatin immunoprecipitation-guided ligation and selection (ChIP-GLAS) identified binding of SND1 to the promoter region of several members of the TGFβ signaling pathway and it was documented that overexpression of SND1 augmented expression of the corresponding mRNAs [31]. However, whether TGFβ itself is regulated by SND1 was not addressed in that study. We document that SND1-induced AT1R activation increases TGFβ expression. Our microarray studies identified downregulation of TGFβ downstream genes in SND1-knockdown clones compared to control clones. Additionally, our previous protein array studies identified regulation of TGFβ downstream proteins, such as PAI-1 and IGFBP3, by SND1 [12]. We employed PAI-1 as a read-out of SND1–AT1R–TGFβ function because of its known role in regulating migration, invasion and angiogenesis [27]. However, it might be the concerted efforts of multiple TGFβ downstream genes that bring forth the profound phenotypic effect observed upon SND1 manipulation.

AT1R activation by SND1 leads to activation of ERK and SMAD2 signaling that might exert both TGFβ-mediated and TGFβ-independent effects. Indeed protein array studies reveal that inhibition of ERK abrogated expression of not only PAI-1 and IGFBP3 but also TIMP-1 and IL-8, known targets of AngII/AT1R signaling, markedly [13]. Inhibition of ERK resulted in significant inhibition of migration and invasion by human HCC cells. ERK activation plays a pivotal role in hepatocarcinogenesis and activated ERK is a potential tissue biomarker for HCC [32]. Our observation linking SND1 overexpression with ERK activation confers added importance to the regulatory role of SND1 in HCC development and progression.

Our current and previous studies reveal that SND1 activates multiple pro-oncogenic signaling, such as NF-κB, AngII/AT1R, ERK and TGFβ. Removal of Smad2, AP-1 and NF-κB binding sites from PAI-1 promoter profoundly abrogated PAI-1 promoter activity in

SND1-overexpressing clones suggesting that PAI-1 expression itself might be regulated by multiple signaling pathways activated by SND1. SND1 thus might be a nodal point in hepatocarcinogenesis and SND1 inhibitors might serve as novel and effective therapeutic approach for HCC.

Conflict of interest

All authors declare that no conflict of interest exists.

Acknowledgements

The present study was supported in part by Grants from the James S. McDonnell Foundation and National Cancer Institute Grant R01 CA138540 (D.S.) and NIH Grant R01 CA134721 (P.B.F.). P.B.F. holds the Thelma Newmeyer Corman Chair in Cancer Research and is a SWCRF Investigator. D.S. is the Harrison Endowed Scholar in Cancer Research and a Blick scholar. The authors declare no conflict of interest.

Appendix A. Supplementary data

Supplementary data associated with this article can be found, in the online version, at http://dx.doi.org/10.1016/j.fob.2014.03.012.

References

[1] Parkin, D.M., Bray, F., Ferlay, J. and Pisani, P. (2005) Global cancer statistics, 2002. CA Cancer J. Clin. 55, 74–108.
[2] Siegel, R., Naishadham, D. and Jemal, A. (2012) Cancer statistics, 2012. CA Cancer J. Clin. 62, 10–29.
[3] Llovet, J.M. and Bruix, J. (2008) Molecular targeted therapies in hepatocellular carcinoma. Hepatology 48, 1312–1327.
[4] Llovet, J.M., Burroughs, A. and Bruix, J. (2003) Hepatocellular carcinoma. Lancet 362, 1907–1917.
[5] Marchesini, G. et al. (2001) Nonalcoholic fatty liver disease: a feature of the metabolic syndrome. Diabetes 50, 1844–1850.
[6] Li, C.L., Yang, W.Z., Chen, Y.P. and Yuan, H.S. (2008) Structural and functional insights into human Tudor-SN, a key component linking RNA interference and editing. Nucleic Acids Res. 36, 3579–3589.
[7] Tong, X., Drapkin, R., Yalamanchili, R., Mosialos, G. and Kieff, E. (1995) The Epstein–Barr virus nuclear protein 2 acidic domain forms a complex with a novel cellular coactivator that can interact with TFIIE. Mol. Cell. Biol. 15, 4735–4744.
[8] Tsuchiya, N., Ochiai, M., Nakashima, K., Ubagai, T., Sugimura, T. and Nakagama, H. (2007) SND1, a component of RNA-induced silencing complex, is up-regulated in human colon cancers and implicated in early stage colon carcinogenesis. Cancer Res. 67, 9568–9576.
[9] Blanco, M.A., Aleckovic, M., Hua, Y., Li, T., Wei, Y., Xu, Z., Cristea, I.M. and Kang, Y. (2011) Identification of staphylococcal nuclease domain-containing 1 (SND1) as a Metadherin-interacting protein with metastasis-promoting functions. J. Biol. Chem. 286, 19982–19992.
[10] Kuruma, H. et al. (2009) Staphylococcal nuclease domain-containing protein 1 as a potential tissue marker for prostate cancer. Am. J. Pathol. 174, 2044–2050.
[11] Yoo, B.K. et al. (2011) Increased RNA-induced silencing complex (RISC) activity contributes to hepatocelllular carcinoma. Hepatology 53, 1538–1548.
[12] Santhekadur, P.K. et al. (2012) Multifunction protein staphylococcal nuclease domain containing 1 (SND1) promotes tumor angiogenesis in human hepatocellular carcinoma through novel pathway that involves nuclear factor kappaB and miR-221. J. Biol. Chem. 287, 13952–13958.
[13] Kaji, K., Yoshiji, H., Ikenaka, Y., Noguchi, R., Aihara, Y., Shirai, Y., Douhara, A. and Fukui, H. (2012) Possible involvement of angiogenesis in chronic liver diseases: interaction among renin–angiotensin–aldosterone system, insulin resistance and oxidative stress. Curr. Med. Chem. 19, 1889–1898.
[14] Friedman, S.L. (2003) Liver fibrosis – from bench to bedside. J. Hepatol. 38 (Suppl. 1), S38–S53.
[15] Bataller, R. et al. (2000) Angiotensin II induces contraction and proliferation of human hepatic stellate cells. Gastroenterology 118, 1149–1156.
[16] Itabashi, H. et al. (2008) Angiotensin II and epidermal growth factor receptor cross-talk mediated by a disintegrin and metalloprotease accelerates tumor cell proliferation of hepatocellular carcinoma cell lines. Hepatol. Res. 38, 601–613.
[17] Perlman, A., Lawsin, L.M., Kolachana, P., Saji, M., Moore Jr., J. and Ringel, M.D. (2004) Angiotensin II regulation of TGF-beta in murine mesangial cells involves both PI3 kinase and MAP kinase. Ann. Clin. Lab. Sci. 34, 277–286.
[18] Katsuno, Y., Lamouille, S. and Derynck, R. (2013) TGF-beta signaling and epithelial–mesenchymal transition in cancer progression. Curr. Opin. Oncol. 25, 76–84.
[19] Yoshiji, H. et al. (2009) Losartan, an angiotensin-II type 1 receptor blocker, attenuates the liver fibrosis development of non-alcoholic steatohepatitis in the rat. BMC Res. Notes 2, 70.
[20] Jonsson, J.R., Clouston, A.D., Ando, Y., Kelemen, L.I., Horn, M.J., Adamson, M.D., Purdie, D.M. and Powell, E.E. (2001) Angiotensin-converting enzyme inhibition attenuates the progression of rat hepatic fibrosis. Gastroenterology 121, 148–155.
[21] Yoshiji, H. et al. (2009) Combination of vitamin K2 and angiotensin-converting enzyme inhibitor ameliorates cumulative recurrence of hepatocellular carcinoma. J. Hepatol. 51, 315–321.
[22] Yoo, B.K. et al. (2009) Astrocyte elevated gene-1 regulates hepatocellular carcinoma development and progression. J. Clin. Invest. 119, 465–477.
[23] Vayalil, P.K., Iles, K.E., Choi, J., Yi, A.K., Postlethwait, E.M. and Liu, R.M. (2007) Glutathione suppresses TGF-beta-induced PAI-1 expression by inhibiting p38 and JNK MAPK and the binding of AP-1, SP-1, and Smad to the PAI-1 promoter. Am. J. Physiol. Lung Cell. Mol. Physiol. 293, L1281–L1292.
[24] Santhekadur, P.K. et al. (2012) Late SV40 factor (LSF) enhances angiogenesis by transcriptionally up-regulating matrix metalloproteinase-9 (MMP-9). J. Biol. Chem. 287, 3425–3432.
[25] Yoo, B.K. et al. (2010) Transcription factor late SV40 factor (LSF) functions as an oncogene in hepatocellular carcinoma. Proc. Natl. Acad. Sci. USA 107, 8357–8362.
[26] Untergasser, G., Gander, R., Lilg, C., Lepperdinger, G., Plas, E. and Berger, P. (2005) Profiling molecular targets of TGF-beta1 in prostate fibroblast-to-myofibroblast transdifferentiation. Mech. Ageing Dev. 126, 59–69.
[27] Dass, K., Ahmad, A., Azmi, A.S., Sarkar, S.H. and Sarkar, F.H. (2008) Evolving role of uPA/uPAR system in human cancers. Cancer Treat. Rev. 34, 122–136.
[28] Paukku, K., Kalkkinen, N., Silvennoinen, O., Kontula, K.K. and Lehtonen, J.Y. (2008) P100 increases AT1R expression through interaction with AT1R 3′-UTR. Nucleic Acids Res. 36, 4474–4487.
[29] Caudy, A.A. et al. (2003) A micrococcal nuclease homologue in RNAi effector complexes. Nature 425, 411–414.
[30] Chen, R.H., Ebner, R. and Derynck, R. (1993) Inactivation of the type II receptor reveals two receptor pathways for the diverse TGF-beta activities. Science 260, 1335–1338.
[31] Liu, X. et al. (2011) Identification of p100 target promoters by chromatin immunoprecipitation-guided ligation and selection (ChIP-GLAS). Cell. Mol. Immunol. 8, 88–91.
[32] Villanueva, A., Newell, P., Chiang, D.Y., Friedman, S.L. and Llovet, J.M. (2007) Genomics and signaling pathways in hepatocellular carcinoma. Semin. Liver Dis. 27, 55–76.